Magnetic properties of He^+-irradiated Pt/Co/Pt ultrathin films

T. Devolder,[1,*] J. Ferré,[2] C. Chappert,[1] H. Bernas,[3] J.-P. Jamet,[2] and V. Mathet[1]
[1]*Institut d'Electronique Fondamentale, CNRS UMR 8622, Université Paris XI, 91405 ORSAY Cedex, France*
[2]*Laboratoire de Physique des Solides, CNRS UMR 8502, Université Paris XI, 91405 ORSAY Cedex, France*
[3]*Centre de Spectroscopie Nucléaire et de Spectroscopie de Masse, CNRS UPR 6412, Université Paris XI, 91405 ORSAY Cedex, France*
(Received 2 February 2001; published 23 July 2001)

We have used ion irradiation to modify the perpendicular magnetic anisotropy and the magnetic coercivity of ultrathin Pt/Co(5 Å)/Pt films without affecting their surface roughness. By studying the magnetization-reversal mechanisms at various temperatures, we show that ion irradiation does not alter the high lateral homogeneity of the films: magnetization reversal still occurs by very few nucleation events followed by easy domain-wall motion. We discuss the reason why irradiation actually reduces the density of sites effectively pinning the domain walls during magnetization reversal: the significant increase in domain-wall-propagation activation volume indicates that the defects created by irradiation are too densely packed to influence the domain-wall-propagation mode. We also show that ion irradiation reduces the Curie temperature and may lower it below 300 K. The temperature dependence of the magnetization of the films irradiated at fluences below $2\times10^{16}\,He^+/cm^2$ indicates a two-dimensional system with an Ising-type exchange Hamitonian. For higher irradiation fluences, the easy axis of magnetization tilts towards an easy cone and the films exhibit paramagnetic behavior at 300 K. The ability to adjust the magnetic technical properties via irradiation indicates that He^+ irradiation could be of great interest for applications in thin-film magnetism.

DOI: 10.1103/PhysRevB.64.064415 PACS number(s): 75.70.Cn, 75.50.Ss

I. INTRODUCTION

Ion-assisted techniques—''ion engineering''—are widely used in material science to tune a variety of physical properties. Among these techniques, sputter deposition, ion milling, implantation, surface treatment, and ion-beam mixing are of major technological importance. Silicon, silica, and more generally semiconductor processing is by far the major customer of ion engineering. The applications of post-growth ion bombardment to magnetic metals are still limited. Ion-beam mixing has been used for producing metastable[1] or amorphous alloys[2] with atomic ratio corresponding to those of the initial constituent layers. Alternatively, changes in roughness of thin magnetic films[3] have been used for altering their transport properties.

Otherwise, irradiation-induced changes in micromagnetic properties have been used very little. The reason seems that the relevant fundamental lengths involved in thin-film micromagnetics are nanometric (e.g., the exchange length, the Bloch wall width) or even quasi-atomic (magnetic anisotropy) so that ion-assisted techniques may only be of interest for thin-film magnetism if they imply a true control of the underlying physical processes with atomic precision.

In Ref. 4, we showed that adapting ion mixing to ultrathin metallic films would require rare and short-range ion-induced atomic displacements. Based on this study, we have developed a patterning method for ultrathin Pt/Co(5–20 Å)/Pt sandwiches whose magnetic anisotropy depends sensitively on the Co-Pt interface states: the more abrupt the interfaces are, the higher the magnetic anisotropy. The main concepts of the patterning process are discussed in Ref. 4: by irradiating the film with 30-keV He^+ (*light*) ions, we gradually roughen its Co/Pt interfaces, reducing the anisotropy and hence the coercive force and the Curie temperature in a controlled way.

This study stimulated research devoted to the fundamental understanding needed for a realistic assessment of the technological potential of the magnetic-film irradiation. We have outlined the phenomena governing the interaction of the ion beam with the magnetic materials, and discussed the resulting structural changes.[5] Anisotropy was reviewed by Weller *et al.*,[6] while the applications to magnetic patterning and information storage were discussed by various groups in Refs. 7 and 8.

Here we focus on the so-called ''technical'' magnetic properties—coercivity, magnetization reversal mechanism, Curie temperature—in uniformly irradiated ultrathin sandwiches. By studies of hysteresis loops at low temperature and of the critical behavior near T_C we correlate the magnetization-reversal processes to the samples' microstructure. This paper follows and complements a preliminary report by Ferré *et al.*[9]

We have presently limited our study to sputter-grown ultrathin Pt/Co ($t_{Co}\approx5$ Å)/Pt films on $Al_2O_3(0002)$ single crystals, irradiated with 30-keV He^+ ions at fluences up to $10^{17}\,He^+/cm^2$. Their structural characteristics are reported elsewhere.[5] Their microstructure consists of (111) textured twin-domain grains of size 30–40 nm. Neither crystallographic texture nor grain size are affected by irradiation, wherein the ions are implanted deep into the substrate. As a result of the quite low sputtering rate (0.12 at./ion), the rms surface roughness increases slightly. Atomic-force microscopy indicates that it increases from 2.1 Å before irradiation to 2.6 Å after a fluence of $3\times10^{16}\,He^+/cm^2$.

II. HYSTERESIS PROPERTIES AT ROOM TEMPERATURE

We first recall and extend the results of Ref. 9 on static coercivity (Sec. II A) and then study the magnetization-reversal mechanism in Sec. II B.

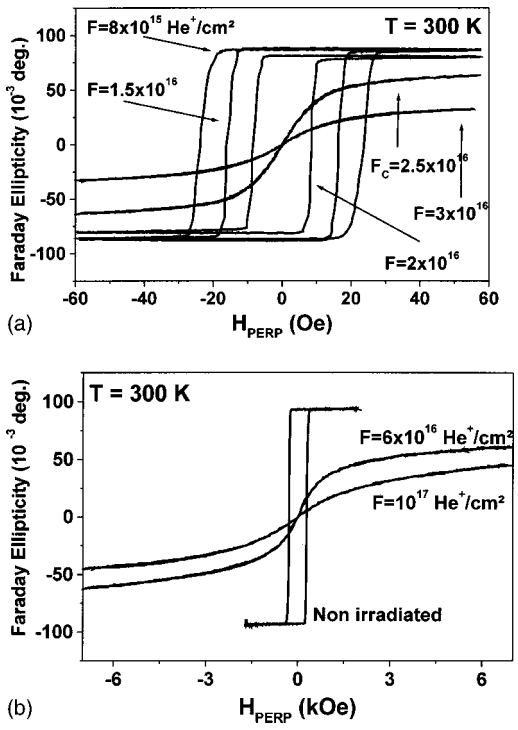

FIG. 1. Polar magneto-optical Faraday-effect hysteresis loops of Pt/Co(5 Å)/Pt/Al_2O_3 films. The loops are measured with strictly identical sweeping rates in each plot. (a) After medium irradiation fluences. (b) Before irradiation and after high fluences.

A. Static properties at room temperature

Figure 1 displays the magneto-optical Faraday ellipticity versus the magnitude of a field applied perpendicular to the film plane. The Faraday ellipticity is proportional to the magnetization perpendicular component $M_\perp$, with a proportionality ratio depending on the structure but not on the temperature. Before irradiation, the easy axis lies along the normal of the film and the magnetization-reversal mechanism occurs through very few nucleation events, followed by easy domain-wall (DW) propagation.[10] Irradiation first gradually reduces the coercive force, while maintaining the square shape of the loop (Fig. 1), i.e., the domain-wall propagation-induced magnetization reversal.[9] Previous studies[11,5] have shown that this evolution correlates with a reduction of the magnetocrystalline anisotropy parameters K_1 and K_2, which are defined by the usual form of total anisotropy energy,

$$E_{\mathrm{tot}}=(-2\pi M_S^2+K_1)\sin^2\theta+K_2\sin^4\theta, \qquad (1)$$

where θ is the angle between the magnetization and the sample-surface normal. $-2\pi M_S^2$ is the macroscopic-shape anisotropy term. K_1 and K_2 measurement relies on hard-axis hysteresis loop fitting.[5] In our Pt/Co (5 Å)/Pt case, the initial K_1 and K_2 are 13×10^6 and 0.8×10^6 erg/cm^3, respectively. While K_1 drops continuously to 7×10^6 erg/cm^3 as the fluence rises to 2×10^{16} He$^+$/cm^2, K_2 stabilizes near 0.35×10^6 erg/cm^3 when the fluence reaches 8×10^{15} He$^+$/cm^3.

After a critical ion fluence $F_C=2.5\times10^{16}$ He$^+$/cm^2, the remanent magnetization vanishes and the loop becomes fully reversible [Fig. 1(b)] at room temperature: its Langevin functional shape indicates a paramagnetic state with large magnetic susceptibility χ. The Curie point (T_C) is then just below room temperature. The susceptibility χ goes on diminishing for $F>F_C$, indicating that the T_C decreases further.

B. Dynamic properties at room temperature

Figure 2 displays some representative magnetic after-effect studies on perpendicularly magnetized films. The measurement procedure is the following: we first drive the sample into a single-domain state, then abruptly reverse the applied perpendicular field and measure the resulting evolution of $M_\perp$. Before and after irradiation, the initial curvature and horizontal slope of the sample response indicate[12] that the volume where magnetization reverses through nucleation events is always a negligible fraction ($<10^{-4}$) of the total magnetic area. Although not exhaustive, our magnetic-imaging studies[9] suggest that typically less than one nucleation event per mm^2 occurs. This indicates that the energy barriers for nucleation are higher than that of reversed-domain expansion by DW motion: the nucleation field H_N is greater than the propagation field H_P. Using magneto-optical microscopy with 0.4 μm resolution, we have also shown[9] that DW propagation occurs without change of wall curvature from micrometer scales to at least millimeter scales, and hence that the dispersion in DW-motion energy barriers is low. Even after irradiation, the propagation field H_P does not vary significantly over the sample.

In addition, a clear feature of Fig. 2 is that magnetization reversal starts after a given time delay $t_{\mathrm{delay}}(H)$ in the probed area. Say $t_{1/2}(H)$ is the time needed for half switching [i.e., $M_\perp(t_{1/2})=0$ and $M_\perp(t\leqslant t_{\mathrm{delay}})>0.95$]. Figure 2(c) indicates that t_{delay} and $t_{1/2}$ are proportional. Magnetization reversal in the probed area occurs thus through DW motion after a nucleation event *outside* the probed area, t_{delay} being the time needed for the wall to reach the probed area.[13] More quantitatively, a major point of Fig. 2 is that the after-effect curves are invariant[14] by a scaling factor $[H/\ln(t)]$. We can thus write the usual[15] Arrhenius law for the DW velocity,

$$v=v_0\exp[-E_p-2M_S\times t_{\mathrm{Co}}l_B^2H)/k_BT],$$

where E_p is an energy barrier, l_B is the Barkhausen length, i.e., the typical extension of the elementary jumps of a propagating DW. The Barkhausen length l_B is a convolution of the wall width and of the typical distance between the DW friction centers: The higher the l_B, the less numerous the defects affecting DW velocity. Since the entire surface magnetization is reversed by DW motion, the time needed for half switching $t_{1/2}(H)$ is such that $\ln(t_{1/2})$ is a line of slope $-2M_Sl_B^2t_{\mathrm{Co}}$.

We determined l_B using the data of Fig. 2. l_B is 38 nm before irradiation and it increases significantly to 61 nm after an irradiation fluence of 10^{16} He$^+$/cm^2. This means that irradiation reduces the density of effective pinning sites. Since the number of irradiation-induced defects certainly increases, this means that the relation between this damage and the physical properties relevant to DW propagation is not straightforward. The enhanced uniformity of the defect dis-

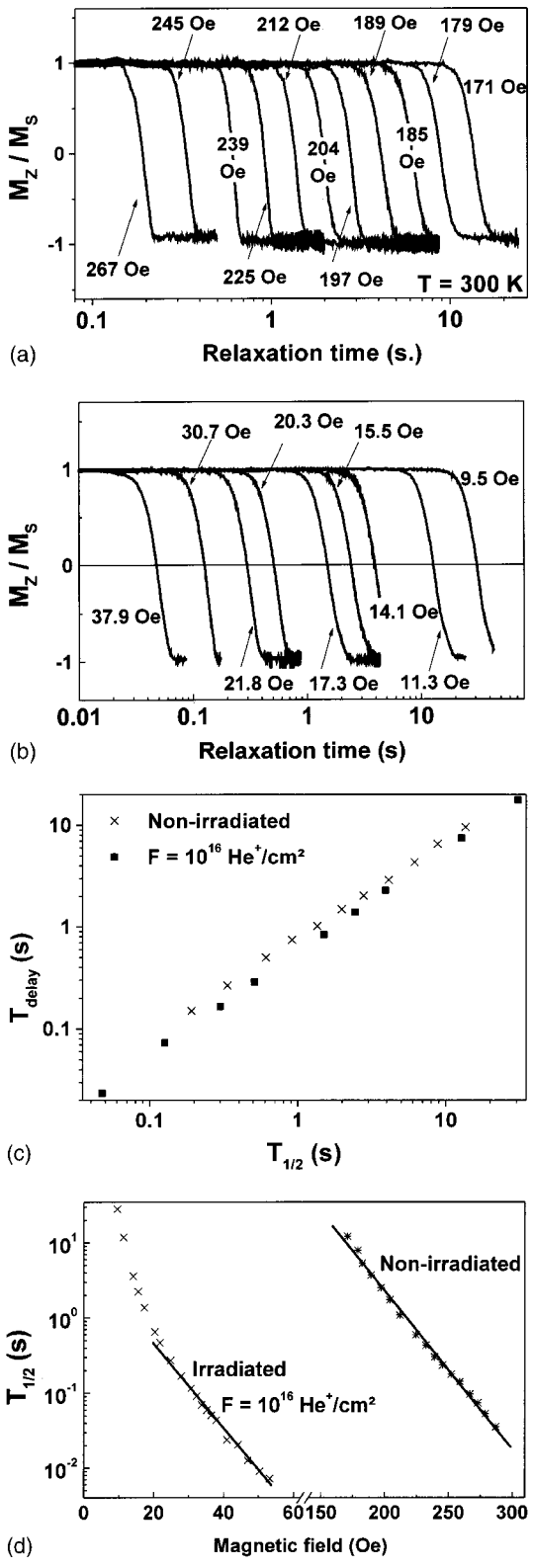

FIG. 2. Magnetic relaxation of Pt/Co(5 Å)/Pt/Al_2O_3 films after application of reverse fields of different magnitudes. (a) Before irradiation, (b) After $F=10^{16}\,He^+/cm^2$ irradiation. (c) Correlation between t_{delay} (start of the relaxation phenomenon) and $t_{1/2}$ (time for half switching): they are proportional in the whole studied field interval. (d) Correlation between $\ln(t_{1/2})$ and the applied field H, before and after $F=10^{16}\,He^+/cm^2$ irradiation.

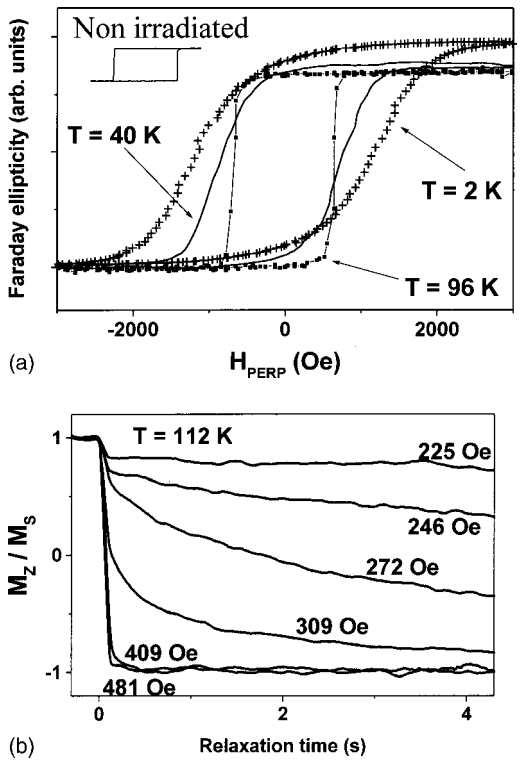

FIG. 3. (a) Hysteresis loops versus temperature for a $F=1.5\times10^{16}\,He^+/cm^2$-irradiated Pt/Co(5 Å)/Pt/Al_2O_3 film. Inset: Before irradiation, the loop is square with a coercivity of 1.9 kOe at 2 K. (b) Magnetic relaxation at 112 K measured on a Pt/Co(5 Å)/Pt/SiO_2 film irradiated at $F=10^{16}\,He^+/cm^2$.

tribution is apparently a crucial factor in reducing their DW-pinning efficiency, as we shall discuss in Sec. IV B.

Our main—counterintuitive—conclusion is thus that irradiation leads to an increase in the degree of lateral homogeneity of the magnetic properties.

III. THERMAL VARIATION OF THE HYSTERESIS PROPERTIES

In this section, we report how the magnetic properties very with temperature. We first (Sec. III A) focus on a medium-fluence irradiated sample and then determine the easy axes of those sandwiches that are paramagnetic at room temperature. Finally, we detail how the Curie temperature decreases upon irradiation (Sec. III B).

A. Hysteresis below room temperature

The hysteresis loop of the nonirradiated sample is square in the whole temperature interval from 2 to 300 K (see inset in Fig. 3). Whatever the temperature, the easy axis of the nonirradiated sample is perfectly perpendicular to the sample plane and the coercivity is determined by the lowest nucleation field H_N. On the contrary, after irradiation, the remanent ratio $M_{H=0}/M_S$ diminishes while cooling even in those samples that have full remanent magnetization at 300 K. Figure 3(a) displays the representative case of a $F=1.5\times10^{16}\,He^+/cm^2$ irradiated sandwich. Between 96 and 300 K,

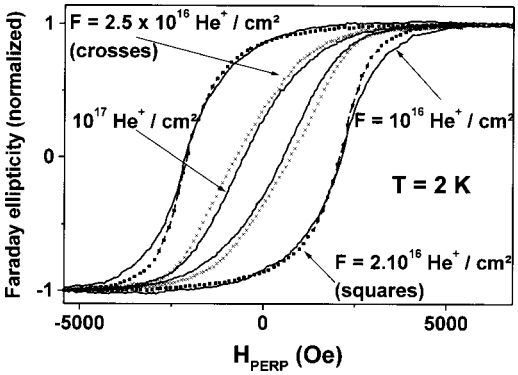

FIG. 4. Hysteresis loops at $T=2$ K of some representative Pt/Co(5 Å)/Pt/Al_2O_3 irradiated films.

the loop remains square, with the magneto-optical signal ($\sim M_S$) decreasing with increasing temperature. Below 96 K, M_S increases further, but the remanent magnetization does not. This may arise either from a tilting of the easy magnetization axis or from the spontaneous nucleation of oppositely magnetized domains as a result of strong internal dipolar coupling. The second hypothesis can be ruled out because the initial—positive field—part of the loops was determined to be reversible. We suggest that while cooling, the increasing magnetization enhances the shape anisotropy, which finally overtakes the magneto-crystalline anisotropy thus triggering a tilt of the easy magnetization axis towards an easy cone of low angular aperture $\sim 32°$. The large K_2 maintains a large perpendicular component even if $K_1 \approx 2\pi M_S^2$. Low-temperature longitudinal magneto-optical Kerr-effect experiments in perpendicular applied field would be required to confirm this interpretation.

Another main point of Fig. 3(a) is the pronounced rounding of the hysteresis loop near H_C at low temperatures $T \leqslant 40$ K. This indicates[16] that the magnetization reversal no longer occurs by easy DW propagation below this temperature. This is confirmed by the $T=112$ K magnetic after-effect study reported in Fig. 3(b): the relaxation curves are now convex both before and after $t_{1/2}$. The absence of any inflection is a strong indication[14] that most of the magnetic volume is now reversed by nucleation events. In conclusion, low temperatures inhibit the DW propagation, and in contrast with $T=300$ K, the propagation field H_P becomes higher than the nucleation field H_N. For $F=1.5\times10^{16}$ He^+/cm^2, the $\{H_N, H_P\}$ crossing occurs between 40 and 96 K. This observation of $H_N < H_P$ reveals the dispersion in nucleation fields.

To get an insight into the origin of the easy magnetization axis tilting at low temperature, we also studied those irradiated samples that are paramagnetic at room temperature. Both the coercive force and perpendicular magnetization component at 2 K fall very abruptly above $F_C=2.5\times10^{16}$ He^+/cm^2 as shown in Fig. 4: above F_C, the easy magnetization axis undergoes a pronounced reorientation towards an easy cone of magnetization with a very large aperture angle (69° for F_C and 74° for 10^{17} He^+/cm^2).

B. Hysteresis near the Curie temperature

Typical high-temperature hysteresis loops on an irradiated, perpendicularly magnetized sample are displayed in

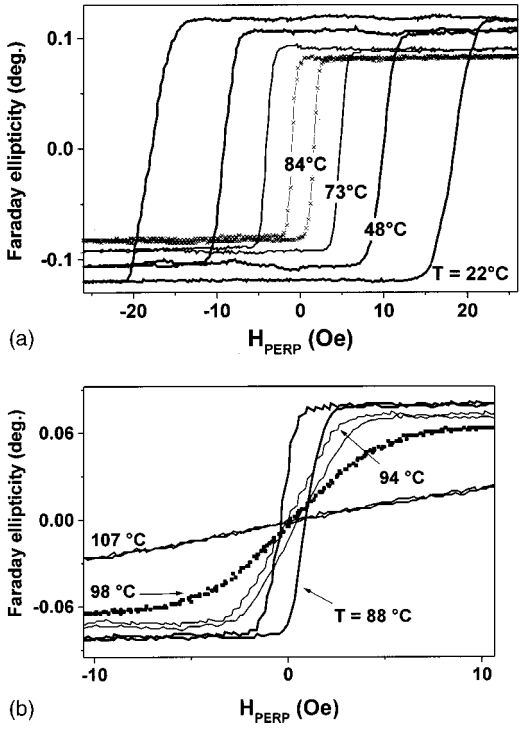

FIG. 5. Hysteresis loops near T_C for a Pt/Co(5 Å)/Pt/Al_2O_3 film irradiated at a fluence of $F=1.5\times10^{16}$ He^+/cm^2. (a) $24\,°C \leqslant T \leqslant 84\,°C$ (b) $88\,°C \leqslant T \leqslant 107\,°C$. Temperatures are given with ± 1 K precision.

Fig. 5. For $F=1.5\times10^{15}$ He^+/cm^2, the loops remain very square as long as $T \leqslant 92\,°C$. The remanent ratio starts falling at 94 °C. The finite coercivity indicates a still ferromagnetic behavior at that temperature. In addition, the loop aspect—back and forth sweeping curves are tilted, straight, and parallel— indicates[17] a perpendicular easy axis with spontaneous nucleation of oppositely magnetized domains.

At 98 °C, the film is paramagnetic. Note that the phase transition takes place in a very narrow temperature interval on the entire centimeter-sized sample, confirming the high lateral homogeneity of the irradiation effect, at least as regards the Curie temperature. The abruptness of the phase transitions after irradiation is demonstrated in Fig. 6. The critical $M(T \leqslant T_C)$ behavior seems to follow a universal variation, with a rather small critical exponent β. Unfortunately, a proper determination of a critical exponent β was not possible because our (magneto-optical) magnetization measurement is nonlocal and averages the magnetization-vector lateral fluctuations over a wide area. For a semiquantitative comparison only, we plotted the perfect two-dimensional Ising model solution $M_\perp \sim (1-T/T_C)^{\beta=1/8}$, which is theoretically the sharpest (smallest β) phase transition possible. Even with our limited precision, it is clear that the three-dimensional (3D) Ising model ($\beta=\frac{5}{16}$) and finite 2D *xy* model ($\beta \approx 0.23$) (Ref. 18) are not abrupt enough to account for the behavior of our perpendicularly magnetized irradiated samples. In the inset to Fig. 6, we also plot the magnetic susceptibility χ for $F=2\times10^{16}$ He^+/cm^2 above $T_C=340\pm1$ K. Fitting this dependence with $\chi \sim (1-T/T_C)^{-\gamma}$ leads to γ values greater than $\frac{7}{4}$, the value pre-

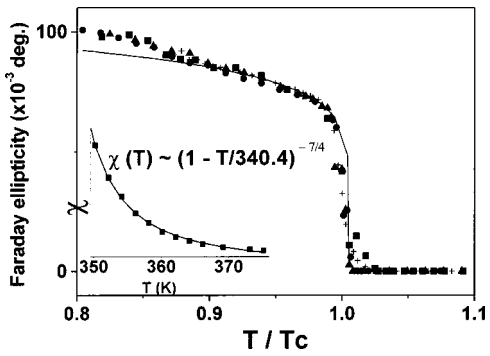

FIG. 6. Ferromagnetic phase transition of perpendicularly magnetized Pt/Co(5 Å)/Pt/Al_2O_3 films irradiated at respectively, $F=2\times10^{16}$ (cross symbols); 1.5×10^{16} (squares); 10^{16} (circles); 8×10^{15} He^+/cm^2 (triangles). Bold line: phase transition for a 2D Ising model. Inset: magnetic susceptibility above T_C for $F=2\times10^{16}$ He^+/cm^2 and corresponding 2D Ising model fit with $\gamma=7/4$ and $T_C=340.4$ K.

dicted for two-dimensional Ising systems. From scaling theory,[19] any geometrical space of higher dimension and any order parameter with more degrees of freedom would lead to a lower γ, in contradiction with our susceptibility measurements.

The manner in which the Curie temperature decreases upon irradiation is shown in Fig. 7.[20] T_C first diminishes slowly for $F\leqslant F_C$, then falls quite abruptly near F_C and finally stabilizes just below room temperature. It seems that the easy-axis reorientation towards an easy plane correlates with a significant T_C decrease. We discuss this point in the next section.

IV. DISCUSSION

We shall first discuss the correlation between the reorientation of the easy magnetization axis and the lowering of T_C at the fluence $F_C=2.5\times10^{16}$ He^+/cm^2 in Sec. IV A. We then analyze the surprisingly high lateral homogeneity of the irradiated samples as regards dynamic properties (Sec. IV B) by enumerating the types of DW pinning centers that may be affected or created by the Helium irradiation.

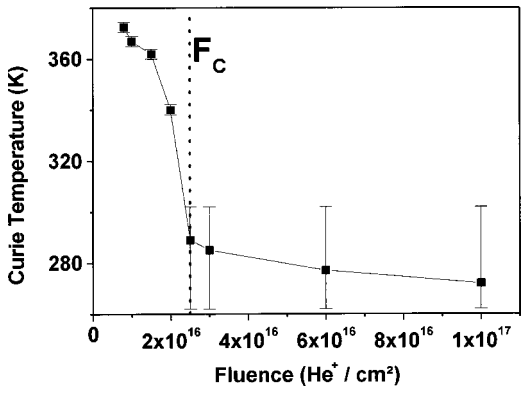

FIG. 7. Curie temperature of He^+ irradiated Pt/Co(5 Å)/Pt/Al_2O_3 films versus ion fluence. F_C is the fluence required to induce a paramagnetic behavior at room temperature.

A. Curie temperature

Thermal magnetization fluctuations (spin waves) act to destroy ferromagnetic ordering when the temperature of such a system is increased to T_C. Magnetocrystalline anisotropy holds the magnetization vector along a given direction and thus helps the exchange interaction to limit these fluctuations, especially in 2D systems.[21] In perpendicularly magnetized samples ($F\leqslant F_C$), the diminution of T_C could thus arise from the gradual lowering of the anisotropy.

However, structural studies[22] have shown that helium irradiation both decreases the Co-Co bond length and the number of Co-Co neighbors. It is thus likely that the Co-Co pair-exchange energy increases, which should increase T_C and that at the same time the number of Co-Co bonds decreases, which should reduce T_C. This complexity limits our understanding of the behavior of T_C below F_C.

The magnetic evolution near F_C may arise from clearer reasons: the easy-axis reorientation transition is so abrupt that the pair-exchange energy, and the Co-Co coordination number may be assumed as almost constant around F_C. When perpendicularly magnetized, the dimensionality of the sample's order parameter—the magnetization vector—is 1. After the magnetization reorientation at F_C, the magnetization vector can vary along an easy cone so that the dimensionality of the order parameter is raised to 2. From phase-transition theories, it is well known that the ordering temperature decreases as the dimensionality of the order parameter increases, i.e., as the number of fluctuation degrees of freedom increases. In summary, the ion-induced reorientation of the easy magnetization axis increases the order-parameter dimensionality, thus triggering a significant reduction of T_C.

B. Relation between irradiation-induced disorder and dynamic magnetic properties

For a realistic assessment of the potential of modifying the magnetic anisotropy by irradiation, we need to determine whether it can be generalized to other material. We therefore need to understand the surprisingly high lateral homogeneity of the irradiated samples as regards dynamic properties. A very important point is that helium irradiation reduces the effective density of DW propagation-pinning centers (Sec. II B). The pinning centers may be any source of lateral nonhomogeneity in a magnetic property: grain boundaries, cobalt terrace steps, roughness, short- or long-range fluctuations of cobalt thickness or film strain. We have shown elsewhere[23] that the grain size was not affected by helium irradiation. We also showed that most atomic displacements involved in the irradiation-induced mixing process are very small, typically 2–5 Å.[5,24] As a result, no extended defect such as grain-boundary or long-range cobalt-thickness fluctuations can disappear in the irradiation process. These defects must still pin the DW in the irradiated samples.

In contrast, the cobalt terrace steps are strongly modified by irradiation. A fluence of 10^{16} ions/cm^2 induces a Co/Pt interface intermixing that corresponds to a roughness slightly greater[5] than the height of the terrace steps (2 Å). These DW-pinning centers are thus likely to play a decreasing role

when increasing the interface roughness by increasing the ion fluence. This gradual blurring of the terrace steps may increase the mean distance between strong pinning centers and thus may explain the irradiation-induced increase of the Barkhausen length.

In perpendicularly magnetized ultrathin films, the DW are Bloch walls having width $\Delta_{\mathrm{Bloch}}=2\sqrt{A/K}$, where A is the exchange stiffness $A\approx 10^{-6}$ erg/cm and the K_1 is as determined above. Thus Δ_{Bloch} is ~6 nm before irradiation and ~15 nm just below F_C. It is well known[25] that the DW are mostly affected by spatial periods of the order of their width Δ_{Bloch}: an isolated defect of size Δ_{Bloch} will be a pinning center but a dense assembly of defects will not pin the DW provided that the defect density is greater than several units per $\Delta^2_{\mathrm{Bloch}}$ surface.

In our samples, the typical irradiation-induced point defect is the substitution of a magnetic atom by a nonmagnetic atom. Because atomic displacements have a typical range[5] of 2–5 Å, all cobalt atoms of a Pt/Co(5 Å)/Pt film may create such point defects.

We may estimate the density of point defects and its fluctuation as introduced by the irradiation process. For this, we consider N atomic substitutions, randomly placed on a macroscopic surface S with mean surface density N/S. A 30-keV He^+ ion induces typically 0.02 displacements per Å of matter traversed.[26] A fluence of 10^{16} ions/cm^2 will thus induce at least $N/S\sim 10$ substitutions/nm^2.

Let us define the probability $P(n)$ of having n atomic substitutions on a small surface $\sigma \ll S$. We define $p=\sigma/S$. This probability follows a binomial law

$$P(n)=\binom{n}{N}p^n(1-p)^{N-n}.$$

It leads to a mean value of n which is $\langle n\rangle = Np$, i.e., the surface area multiplied by the surface density of point defects. The variance of n is

$$\Delta n^2 = Np(1-p).$$

In the limit of small surfaces $\sigma \ll S$, it reduces to $\Delta n^2 = Np$ and the relative fluctuation of defect density is

$$\Delta n/\langle n\rangle = 1/\sqrt{\langle n\rangle}. \qquad (2)$$

Typical local fluctuations of the atomic substitutions density are reported in Table I. For surfaces of size relevant for DW propagation, e.g., $\sigma\sim\Delta^2_{\mathrm{Bloch}}$ and $\sigma\sim l_B^2$, the irradiation-induced density of substitution does not exhibit significant fluctuations.

Thus, the very fact that irradiation induces very numerous substitution defects leads to such large density of the latter that a DW may cover many of them at the same time in its wall width. In summary, the structural disorder introduced by the irradiation process cannot influence the DW propagation mode at room temperature.

TABLE I. Relative fluctuation (%) of point defect density as typically induced by an irradiation fluence of 10^{16} He^+/cm^2. Calculated with Eq. (2).

Surface σ (nm^2)	1×1	5×5	10×10	30×30
Relative fluctuation of point defect density	32%	6%	3%	1%

V. CONCLUSION

30-keV helium-ion irradiation allows us to alter the magnetic anisotropy, and hence the coercivity of Pt/Co(5 Å)/Pt films with perpendicular magnetization, and to induce a paramagnetic transition at room temperature for fluence $F\geqslant F_C = 2.5\times 10^{16}$ He^+/cm^2. Irradiation is a way to fabricate samples with an adjustable Curie point in the room-temperature vicinity. As regards the paramagnetic phase transition, in spite of our limited experimental accuracy, we may conclude that the films irradiated at fluences strictly below F_C exhibit the characteristics of high-quality two-dimensional systems whose exchange interaction is described by an Ising Hamiltonian. At higher irradiation fluences, the easy magnetization axis abruptly tilts towards an easy cone while the correlated change in the order-parameter dimensionality abruptly lowers the Curie temperature.

We have shown that below F_C, magnetization reversal at room temperature occurs through a very limited number of nucleation events followed by easy domain-wall propagation sweeping the whole sample surface. The density of pinning sites is reduced by the irradiation, such that the initial Barkhausen length (38 nm) rises to 61 nm after irradiating at a fluence 10^{16} He^+/cm^2. We showed that the defects created by irradiation are too densely packed to alter the domain-wall-propagation mode. The ability to adjust the magnetic technical properties via irradiation indicates that He^+ irradiation could be of great interest for the thin-film magnetism community.

ACKNOWLEDGMENT

T.D. is grateful to J.-P. Renard for enlighting discussions about Curie temperature in 2D transition metals.

*Corresponding author. FAX: (33) 169154000. Email address: devolder@ief.u-psud.fr

[1] M. Nastasi, L. S. Hung, and J. W. Mayer, Appl. Phys. Lett. **43**, 831 (1983).

[2] G. Choe, R. M. Walser, J. Appl. Phys. **79**, 6306 (1996).

[3] J. Xiao, K. Liu, C. L. Chien, L. F. Schelp, and J. E. Schmidt, J. Appl. Phys. **76**, 6081 (1994).

[4] C. Chappert, H. Bernas, J. Ferré, V. Kottler, J. P. Jamet, Y. Chen, E. Cambril, T. Devolder, F. Rousseaux, V. Mathet, and H. Launois, Science **280**, 1919 (1998); H. Bernas, T. Devolder, C. Chappert, J. Ferré, V. Kottler, Y. Chen, C. Vieu, J.-P. Jamet, V. Mathet, E. Cambril, O. Kaitanov, S. Lemerle, F. Rousseaux, and H. Launois, Nucl. Instrum. Methods Phys. Res. B **148**, 872 (1999); T. Devolder, C. Vieu, H. Bernas, J. Ferré, C. Chappert, J. Gierak, J.-P. Jamet, T. Aign, P. Meyer, Y. Chen, F. Rousseaux, V. Mathet, H. Launois, and O. Kaitanov, C. R. Acad. Sci., Ser. IIb:

Mec., Phys., Chim., Astron. **327**, 925 (1999).
[5] T. Devolder, Phys. Rev. B **62**, 5794 (2000).
[6] D. Weller, J. E. E. Baglin, A. J. Kellock, K. A. Hannibal, M. F. Toney, G. Kusinski, S. Lang, L. Folks, M. E. Best, and B. D. Terris, J. Appl. Phys. **87**, 5768 (2000).
[7] T. Devolder, Y. Chen, C. Chappert, H. Bernas, J. Ferré, J.-P. Jamet, E. Cambril, and H. Launois, J. Vac. Sci. Technol. B **37**, 3117 (1999); T. Devolder, Y. Chen, H. Bernas, C. Chappert, J.-P. Jamet, J. Ferré, and E. Cambril, Appl. Phys. Lett. **74**, 3383 (1999); T. Devolder, C. Chappert, V. Mathet, H. Bernas, Y. Chen, J.-P. Jamet, and J. Ferré, J. Appl. Phys. **87**, 8671 (2000).
[8] B. Terris, L. Folks, D. Weller, J. Baglin, A. Kellock, H. Rothuizen, and P. Vettiger, Appl. Phys. Lett. **75**, 403 (1999); B. Terris, D. Weller, L. Folks, J. E. E. Baglin, and A. Kellock, J. Appl. Phys. **87**, 7004 (2000).
[9] J. Ferré, C. Chappert, H. Bernas, J.-P. Jamet, P. Meyer, O. Kaitanov, S. Lemerle, V. Mathet, F. Rousseaux, and H. Launois, J. Magn. Magn. Mater. **198–199**, 191 (1999).
[10] S. Lemerle, J. Ferré, C. Chappert, V. Mathet, T. Giamarchi, and P. Le Doussal, Phys. Rev. Lett. **80**, 849 (1998).
[11] T. Devolder, H. Bernas, D. Ravelosona, C. Chappert, S. Pizzini, J. Vogel, J. Ferré, J.-P. Jamet, Y. Chen, and V. Mathet, Nucl. Instrum. Methods Phys. Res. B **175-177**, 375 (2001).
[12] Standard model of magnetic after effect in, for instance, M. Labrune, S. Andrieux, F. Rio, and P. Bernstein, J. Magn. Magn. Mater. **80**, 211 (1989).
[13] If the nucleation time t_n was significant, $t_{1/2}$ and t_{delay} would be such that $t_{1/2}=\alpha\ t_{\mathrm{delay}}+t_n$, i.e., not strictly proportional, which is inconsistent with Fig. 2.
[14] This scaling law for the domain-wall velocity is no longer true in the very-low-field regime ($H \ll H_P$), which we could investigate only for the irradiated sample. In this so-called ''creep'' regime [left part of Fig. 2(d)], the velocity follows $v(H) \alpha \exp(H^{1/4})$ breaking the proportionality relation between H and $\ln(t)$. See, e.g., S. Lemerle *et al.*, Phys. Rev. Lett. **80**, 849 (1998).
[15] A. Kirilyuk, J. Ferré, and D. Renard, Europhys. Lett. **24**, 403 (1993); A. Kirilyuk, J. Ferré, J. Pommier, and D. Renard, J. Magn. Magn. Mater. **121**, 536 (1993); A. Kirilyuk, J. Ferré, V. Grolier, J.-P. Jamet, and D. Renard, *ibid.* **171**, 45 (1997).
[16] A. Herpin, *Théorie du Magnétisme* (Presses Universitaires de France, 1964).
[17] For Co/Pt systems, see, e.g., L. Belliard, J. Miltat, V. Kottler, V. Mathet, C. Chappert, and T. Valet, J. Appl. Phys. **81**, 5315 (1997). See also this transition to multidomain formation on perpendicularly magnetized Ni/Cu films near T_C in P. Poulopoulos, M. Farle, U. Bovensiepen, and K. Baberschke, Phys. Rev. B **55**, R11 961 (1997).
[18] F. J. Himpsel, J. E. Ortega, G. J. Mankey, and R. F. Willis, Adv. Phys. **47**, 511 (1998).
[19] G. Toulouse and P. Pfeuty, *Introduction au Groupe de Renormalisation et à ses Applications* (Presses Universitaires de Grenoble, 1975).
[20] It is not possible to perform similar high-temperature measurements on the nonirradiated sample. Its Curie point is indeed above the diffusion threshold of point defects in metals ($\sim$150 °C), so that trying to measure the T_C would anneal the sample and thus change its T_C. See G. Garreau, M. Farle, E. Beaurepaire, and K. Baberschke, Phys. Rev. B **55**, 330 (1997).
[21] P. Bruno, Phys. Rev. B **43**, 6015 (1991); P. Bruno, in *Magnetic Surfaces, Thin Films, and Multilayers*, edited by S. S. P. Parkin *et al.*, MRS Symposia Proceedings No. 231 (Materials Research Society, Pittsburgh, 1991).
[22] EXAFS by T. Devolder, S. Pizzini, J. Vogel, H. Bernas, C. Chappert, V. Mathet, and M. Borowski, Eur. Phys. J. B (to be published).
[23] T. Devolder, Ph.D. thesis, Université Paris-Sud, 2000.
[24] T. Devolder, H. Bernas, D. Ravelosona, C. Chappert, S. Pizzini, J. Vogel, J. Ferré, J.-P. Jamet, Y. Chen, and V. Mathet, Nucl. Instrum. Methods Phys. Res. B (to be published August 2001).
[25] R. Becker and W. Döring, *Ferromagnetismus* (Springer, New York, 1939); L. Néel, *Physica* **15**, 225 (1949).
[26] J. Ziegler, J. Biersack, and U. Littmark, *The Stopping of Ions in Matter* (Pergamon, New York, 1985); Software ''SRIM'' available at http://www.research.ibm.com/ionbeams/home.htm#SRIM